Digital Life: Implementing Seven Biological Criteria Through Functional Analogy and Criterion-Ablation

Anonymous

Abstract

We present a testable integration implementing all seven textbook biological criteria for life—cellular organization, metabolism, homeostasis, growth, reproduction, response to stimuli, and evolution—as functionally interdependent computational processes within a single artificial life system. Existing systems implement at most a subset of these criteria, often as independent modules or static proxies that can be removed without measurable system degradation. Our hybrid swarm-organism architecture implements each criterion as a dynamic process satisfying three conditions—sustained resource consumption, measurable degradation upon removal, and feedback coupling with other criteria—which we term functional analogy. A criterion-ablation experiment (n=30 per condition, seeds held out from calibration) demonstrates that disabling any single criterion causes statistically significant population decline (Mann-Whitney U, Holm-Bonferroni corrected, all $p \leq 0.016$), with Cliff's δ ranging from 0.32 to 1.00. Pairwise ablations reveal sub-additive interactions consistent with shared failure pathways, confirming that criteria damage overlapping subsystems rather than operating independently. A proxy control comparison shows that metabolism implementations of differing complexity produce qualitatively distinct population dynamics, ruling out tautological criterion definitions. The strongest single-ablation effects arise from disabling reproduction (Δ=–89.3%), response to stimuli (Δ=–88.4%), and metabolism (Δ=–84.3%), confirming that these criteria function as necessary, interdependent components of organismal viability rather than decorative labels.

Submission type: Full Paper
Data/Code available at: https://anonymous.4open.science/

Introduction

What distinguishes a living system from a merely complex one? Biology textbooks identify seven criteria—cellular organization, metabolism, homeostasis, growth and development, reproduction, response to stimuli, and evolution (Urry et al., 2020)—but artificial life (ALife) research has struggled to integrate all seven into a single computational system. Most existing platforms implement a subset: evolutionary dynamics without metabolism (Ofria and Wilke, 2004), pattern formation without reproduction (Chan, 2019), or boundary self-organization without evolution (Plantec et al., 2023). Where criteria are nominally present, they often function as simplified proxies—static parameters or independent modules whose removal has no measurable effect on system behavior.

We argue that a meaningful computational model of life requires more than feature checklists. Each criterion must function as a functional analogy of its biological counterpart, satisfying three conditions:

1. Dynamic process: the criterion requires sustained resource consumption at every timestep, not a static lookup.

2. Measurable degradation: ablating the criterion causes statistically significant decline in organism viability.

3. Feedback coupling: the criterion forms at least one feedback loop with another criterion, precluding independent-module implementations.

This definition operationalizes the intuition behind autopoiesis (Maturana and Varela, 1980), the chemoton model's integration of metabolic, boundary, and information subsystems (Gánti, 2003), and minimal-life frameworks (Ruiz-Mirazo et al., 2004) in a form amenable to experimental falsification.

We adopt a weak ALife stance: our system is a functional model of life, not a claim that the organisms are alive. The contribution is methodological—demonstrating that all seven criteria can be integrated as interdependent processes and that their necessity can be rigorously tested.

This paper contributes: (1) a hybrid swarm-organism architecture integrating all seven criteria as function-

ally interdependent processes; (2) an operational definition of functional analogy with three falsifiable conditions; (3) a criterion-ablation methodology demonstrating each criterion's functional necessity with multiple-comparison correction; and (4) pairwise ablation and proxy control experiments characterizing criterion interactions and ruling out tautological definitions. The key contribution is not a new digital organism per se, but a falsifiable experimental framework for testing the functional necessity and interaction of life criteria in any ALife system.

Related Work

Existing ALife systems each excel along different axes of biological fidelity. Tierra (Ray, 1991) and Avida (Ofria and Wilke, 2004) achieve strong evolutionary dynamics but lack spatial bodies and metabolism. Polyworld (Yaeger, 1994) adds NN-driven behavior and single-resource energy budgets. Lenia (Chan, 2019) and Flow-Lenia (Plantec et al., 2023) demonstrate emergent spatial organization in continuous cellular automata, with Flow-Lenia adding mass conservation. ALIEN (Heinemann, 2008) provides a GPU-accelerated particle simulator achieving multi-process interaction on several criteria, though its metabolism uses typed particle interactions rather than a multi-step metabolic network (Level 3 on our rubric). Coralai (Barbieux and Canaan, 2024) combines multi-agent neural cellular automata with energy dynamics but lacks feedback coupling between criteria. No existing system combines multi-step metabolism with active homeostatic regulation.

Theoretically, our framework operationalizes autopoiesis (Maturana and Varela, 1980; McMullin, 2004), extends the chemoton's three-subsystem integration (Gánti, 2003), and enriches NASA's two-criterion definition (Joyce, 1994) following Ruiz-Mirazo et al. (2004). Open-ended evolution metrics (Bedau et al., 2000; Taylor et al., 2016) complement our criterion-ablation approach.

Table 1 summarizes how existing systems score on each criterion using a five-level rubric.

Our system reaches ≥ 4 on five of seven criteria, placing it among the most broadly integrated ALife systems surveyed. We note that these scores are self-assessed; independent evaluation may adjust individual ratings.

System Design

Architecture Overview

The system implements a hybrid two-layer architecture (Figure 1). The outer layer is a continuous toroidal 2D environment (100×100 world units) containing a diffusing resource field. The inner layer consists of 10–50 organisms, each composed of 10–50 swarm agents that collectively maintain the organism's spatial boundary.

Each organism maintains the following runtime state: boundary integrity ($b \in [0, 1]$), metabolic state (energy e, resource r, waste w), internal state vector for homeostatic regulation, a neural-network controller, a genetically encoded metabolic network, age, generation counter, and maturity level.

Seven Criteria Implementation

Table 2 maps each biological criterion to its computational implementation, ablation toggle, and feedback partners.

Cellular organization. Swarm agents collectively define an organism's spatial extent. Boundary integrity b decays each step at a base rate modulated by energy deficit and waste pressure: $\Delta b_{\text{decay}} = -r_b \cdot (1 + s_e \cdot (1 - e) + s_w \cdot w)$, where $r_b = 0.02$ is the base decay rate, $s_e = 0.5$ and $s_w = 0.3$ are scaling factors. Repair occurs proportionally to available energy: $\Delta b_{\text{repair}} = r_r \cdot e \cdot (1 - s_p \cdot w)$, with repair rate $r_r = 0.15$ and waste penalty $s_p = 0.4$. When b falls below a collapse threshold ($b < 0.1$), the organism dies.

Metabolism. Each organism possesses a genetically encoded graph-based metabolic network with 2–4 catalytic nodes and directed edges. The genome segment (16 floats) is decoded via sigmoid mapping: node count $= \text{round}(\sigma(g_0) \cdot 2 + 2)$, catalytic efficiency $= \sigma(g_{2+i}) \cdot 0.9 + 0.1 \in [0.1, 1.0]$, edge existence determined by $|g_j| > 0.3$, and conversion efficiency $= \sigma(g_{13}) \cdot 0.7 + 0.3 \in [0.3, 1.0]$. External resources enter at a designated entry node, flow through the graph with per-edge transfer efficiency in $[0.7, 1.0]$, and exit as energy. Waste accumulates as a byproduct proportional to throughput.

Homeostasis. A feedforward neural network (8 inputs $\rightarrow$ 16 hidden with tanh $\rightarrow$ 4 outputs with tanh; 212 weights) processes sensory inputs (normalized position x, y; velocity v_x, v_y; internal state s_0, s_1, s_2; neighbor density) and produces velocity adjustments and internal-state deltas. The internal state vector enables adaptive regulation: organisms that maintain internal variables within viable ranges survive longer.

Growth and development. Organisms begin as minimal seeds (maturity $m = 0$) and develop toward full capacity ($m = 1$) over time. Maturation gates metabolic throughput and reproductive readiness, ensuring organisms must develop before they can reproduce.

Reproduction. When energy exceeds $e_{\min} = 0.7$ and boundary integrity exceeds $b_{\min} = 0.5$, an organism may divide. The parent pays an energy cost ($c_r = 0.3$),

Table 1: Literature comparison: seven biological criteria scored on a five-level rubric (1=no feature, 2=static parameter, 3=dynamic single process, 4=multi-process interaction, 5=self-maintaining/emergent). Bold indicates scores ≥4.

System	Cell.Org	Metab	Homeo	Growth	Reprod	Response	Evol	Total
Polyworld	2	3	1	1	3	4	4	18
Avida	2	3	1	2	4	3	5	20
Lenia	3	1	2	2	2	3	2	15
ALIEN	4	3	2	3	4	4	4	24
Flow-Lenia	3	3	3	3	3	3	3	21
Coralai	3	3	2	3	3	3	3	20
Ours[†]	4	4	4	3	4	4	3	26

[†]Self-assessment; scores may differ under external evaluation.
Growth (3) and Evolution (3) represent minimum viable implementations satisfying the functional-analogy conditions.
Scores based on published system descriptions; per-criterion justifications available as supplementary material.

Table 2: Mechanism specification: state variables, ablation operators, coupling pathways, and failure modes for each criterion. All criteria satisfy the three functional-analogy conditions (dynamic process, measurable degradation, feedback coupling).

Criterion	State Vars	Ablation	Coupling	Failure
Cell. Org.	$b \in [0,1]$	Skip repair; decay only	$e \to$ repair rate $\to b$	$b<0.1 \to$ death
Metab.	e, r, w; graph $\mathbf{p}$	Freeze (e, r, w)	throughput $\to e \to$ bdry repair	Energy depletion
Homeo.	$\mathbf{s} \in \mathbb{R}^3$	Skip NN delta; decay	$s_0 \to$ repair efficacy	State drift
Growth	$m \in [0,1]$	Freeze m=0	maturity $\to$ reprod. gate	No reproduction
Reprod.	Pop. event	Skip division check	energy cost $\to$ parent e	No replacement
Response	$\mathbf{v}$	Skip velocity delta	movement $\to$ resource $\to r$	Starvation
Evolution	genome $\mathbf{g}$	Copy w/o mutation	$\mathbf{g}$ variation $\to$ all	No adaptation

and the offspring inherits a (possibly mutated) copy of the genome, starting as a seed. Child agents spawn within a radius of the parent's center of mass.

Response to stimuli. The neural-network controller processes a local sensory field each timestep, producing velocity deltas that govern agent movement. Disabling response freezes agents' velocity adjustments, preventing adaptive resource seeking.

Evolution. During reproduction, offspring genomes undergo point mutations (rate = 0.01 per gene, scale = 0.1), reset mutations (rate = 0.001), and scale mutations (rate = 0.005, factor $\in [0.8, 1.2]$). All gene values are clamped to $[-5, 5]$. This produces heritable variation subject to differential survival.

Genome Encoding

The genome is a variable-length vector of 256 floats organized into seven segments: neural-network weights (212), metabolic network (16), homeostasis parameters (8), developmental program (8), reproduction parameters (4), sensory parameters (4), and evolution parameters (4). All criteria are encoded from initialization; segments are activated as features are enabled.

Criterion-Ablation Experiment

This experiment tests whether each of the seven criteria is functionally necessary for organism viability, as predicted by the functional-analogy framework.

Protocol

The system provides seven boolean ablation toggles, one per criterion (e.g., enable_metabolism = false). For each of the seven criteria, we disable that criterion

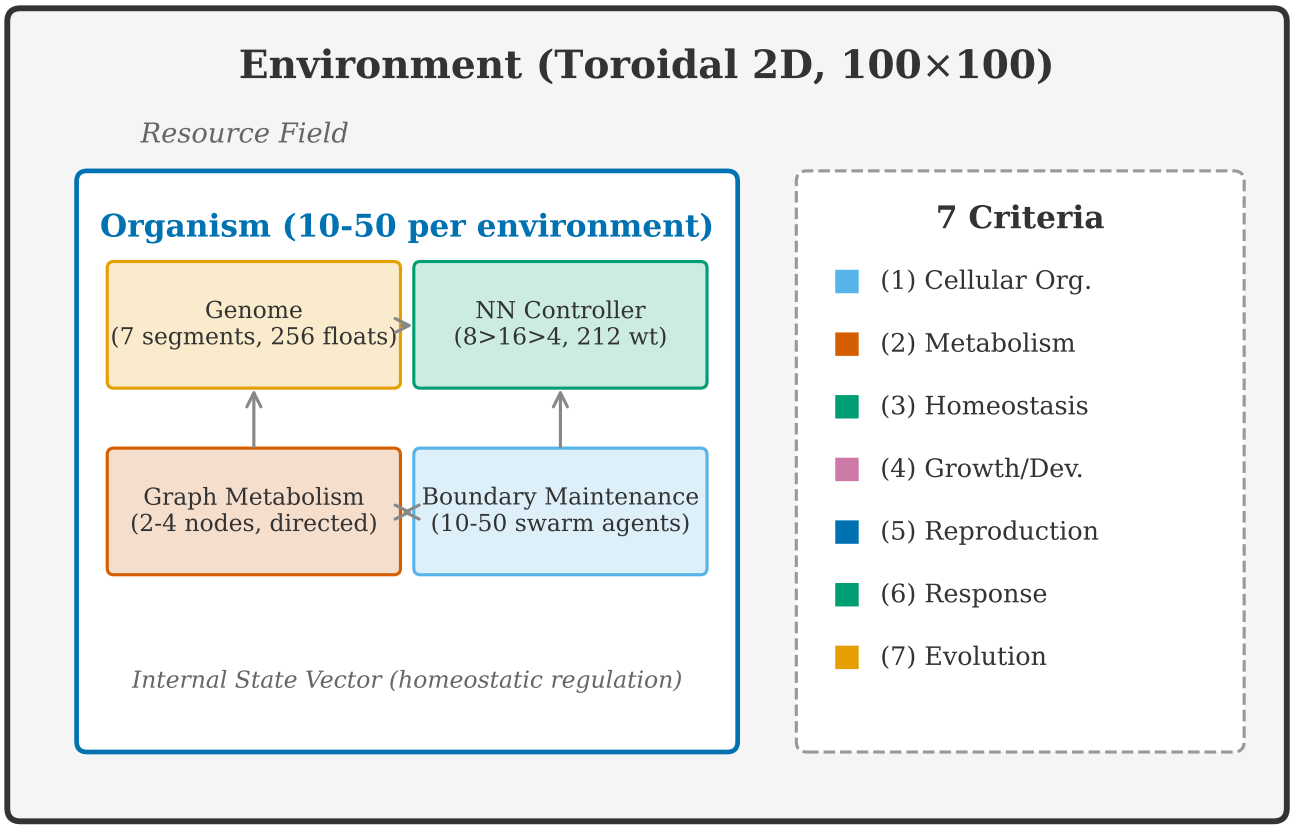

Figure 1: Two-layer architecture. Each organism comprises swarm agents maintaining a spatial boundary, a neural-network controller, a graph-based metabolic network, and a variable-length genome encoding all seven criteria. Organisms inhabit a continuous toroidal environment with a diffusing resource field.

while keeping all others active, and compare the resulting population dynamics against the fully enabled baseline ("normal" condition). This yields eight conditions: one normal baseline and seven single-criterion ablations.

Outcome Measures

An organism is a persistent runtime entity with a unique ID; offspring receive a new ID at division; no merge or split occurs. An organism dies when boundary $b < 0.1$, energy $e \leq 0.0$, or age $> 20{,}000$ steps. The primary dependent variable is N_T, the alive organism count at the final step $T = 2000$; each seed maps to one scalar. Secondary DVs include the area under the alive-count curve (AUC, trapezoidal rule) and median organism lifespan. We additionally report short-horizon viability at $T = 500$ to separate individual survival from population replacement effects.

Data Separation

To prevent overfitting of thresholds, we separate data into:

- Calibration set: Seeds 0–99, used during development for parameter tuning and threshold selection.
- Test set: Seeds 100–129 (n=30), held out until final evaluation. All reported results use this set exclusively.

Calibration confirmed that both metabolism engines produce viable populations (Toy: $\bar{x}$=328.1, Graph: $\bar{x}$=291.8 alive at step 2000). All final experiments use the Graph metabolism engine.

Simulation Parameters

Each simulation runs for 2000 timesteps with population sampled every 50 steps. The environment is a 100×100 toroidal grid with 30 initial organisms, each comprising 25 swarm agents. Resources regenerate at 0.01 per cell per step with no diffusion and toroidal

Table 3: Criterion-ablation results (n=30 per condition). Normal baseline mean: 293.1 (median: 294.5, IQR: 281.5–309.5). δ=Cliff's delta [bootstrap 95% CI]. Seven one-sided tests, Holm-Bonferroni corrected at $\alpha = 0.05$. $^{***}p < 0.001$, $^{*}p < 0.05$.

Condition	Mean	Δ%	δ [95% CI]	p_{corr}	Sig.
No Reprod.	31.3	−89.3	1.00 [1.00, 1.00]	<.001	***
No Response	34.1	−88.4	1.00 [1.00, 1.00]	<.001	***
No Metab.	46.0	−84.3	1.00 [1.00, 1.00]	<.001	***
No Homeo.	68.3	−76.7	1.00 [1.00, 1.00]	<.001	***
No Boundary	121.8	−58.5	1.00 [1.00, 1.00]	<.001	***
No Growth	185.6	−36.7	1.00 [1.00, 1.00]	<.001	***
No Evol.	278.3	−5.1	0.32 [0.02, 0.59]	.016	*

wrap boundary conditions. No early stopping is applied. Ablation toggles do not alter timestep duration or event ordering; disabled processes are simply skipped. Each seed produces a deterministic, reproducible outcome within a given condition, though RNG call sequences differ across conditions when ablated processes (e.g., reproduction) skip conditional RNG draws.

Statistical Design

For each ablation condition, we test the one-sided hypothesis:

$$H_1 : \text{alive\_count}_{\text{normal}} > \text{alive\_count}_{\text{ablated}}$$

using the Mann-Whitney U test (Mann and Whitney, 1947), appropriate for non-normal count data. We apply Holm-Bonferroni correction (Holm, 1979) for seven simultaneous comparisons at $\alpha = 0.05$. Effect sizes are reported as Cliff's δ (Cliff, 1993) for the primary ablation comparisons, with Cohen's d additionally reported for evolution-strengthening experiments to facilitate parametric comparison, with percentile bootstrap 95% confidence intervals (2000 resamples, seed-fixed RNG), appropriate for non-normal distributions.

Results

All seven criterion ablations produce statistically significant population decline compared to the normal baseline (Table 3).

Three ablations cause near-total population collapse (>84% decline): reproduction, response to stimuli, and metabolism. These criteria form the core viability loop—without energy production, adaptive movement, or population renewal, organisms cannot sustain themselves.

Figure 3 shows population trajectories across all conditions. The normal condition (black) stabilizes around 293 organisms by step 1900. Metabolic ablation (orange) causes rapid collapse within the first 200 steps,

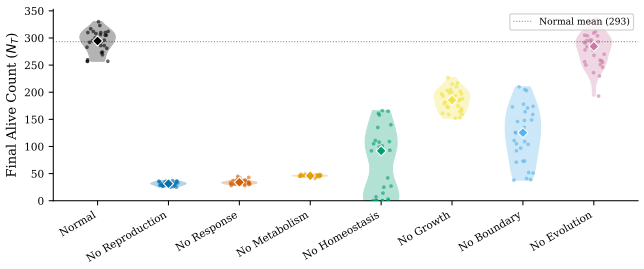

Figure 2: Per-seed distributions of final alive count (N_T) across all conditions (n=30 per condition). Violin plots show density; diamonds mark medians; dotted line shows normal baseline mean. The distribution confirms that ablation effects are consistent across seeds, not driven by outliers.

as organisms cannot produce energy to maintain boundaries. Reproduction ablation (blue) produces a slower but equally terminal decline, as the initial population ages and dies without replacement. Evolution ablation (purple) shows the weakest effect (Cliff's δ=0.32), with populations remaining viable but slightly smaller than normal—consistent with evolution operating as an optimization process rather than a survival necessity at these timescales. AUC of the alive-count curve corroborates N_T rankings across all conditions (normal AUC=435,376 vs. 74,545–412,518 for ablations). Median organism lifespan reveals an individual-vs-population distinction: reproduction-ablated organisms live longer individually (median 751 vs. 132 steps for normal) despite population collapse, confirming that the population decline reflects absent replacement rather than individual fragility. Per-seed distributions are shown in Figure 2.

At $T = 500$ (before long-term population dynamics dominate), reproduction-ablated organisms retain higher survival ($\bar{x}$=47.7 vs. 31.3 at $T = 2000$; normal baseline $\bar{x}_{\text{normal}}$=153.5 at $T = 500$), with 69% decline relative to normal versus 89% at $T = 2000$. This progressive widening confirms that the long-term effect is population-level (no replacement) rather than immediate individual-level failure—organisms can self-maintain without reproduction.

Functional analogy verification. For each criterion, all three conditions are satisfied: (a) each consumes resources per step (energy for boundary repair, metabolic computation, NN evaluation); (b) ablation causes significant degradation (Table 3); and (c) feedback loops are observable (e.g., metabolism ↔ boundary: energy funds repair, boundary collapse stops metabolism). Thus, each criterion qualifies as a functional analogy, not a simplified proxy.

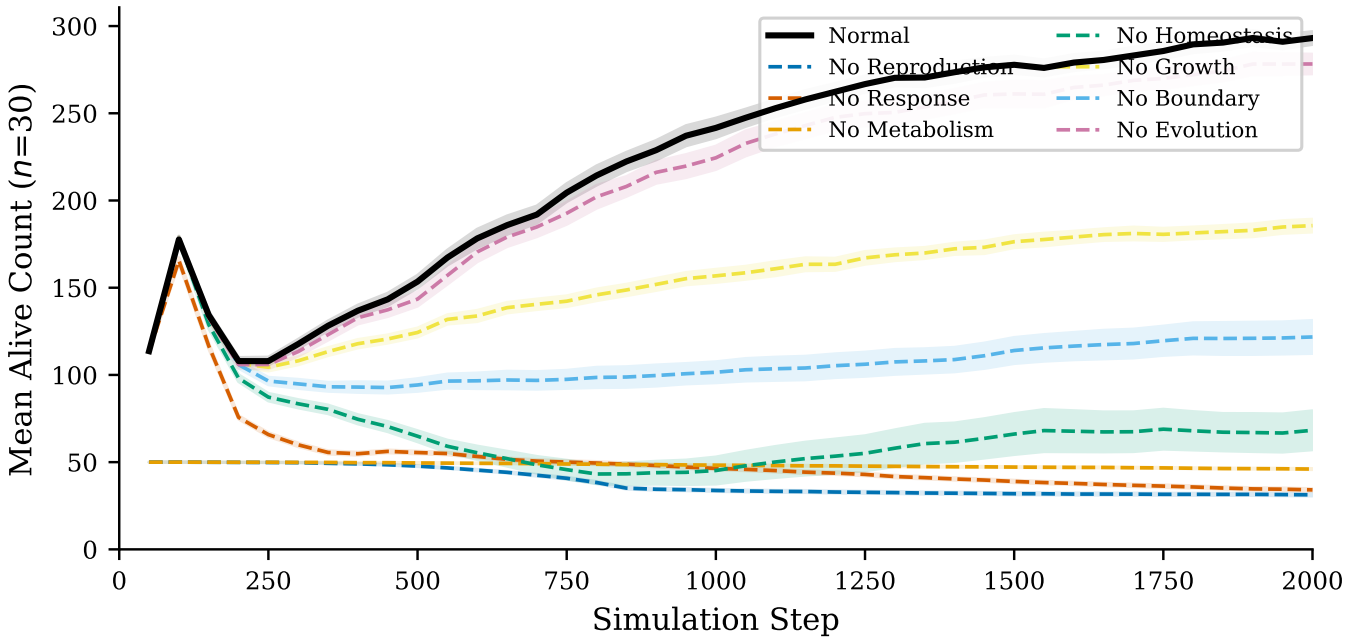

Figure 3: Population dynamics under criterion ablation. Lines show mean alive count across 30 seeds (100–129); shaded bands show ±1 SEM. Normal baseline (thick black) stabilizes near 293 organisms by step 1900. Removing reproduction, response, or metabolism causes >84% population collapse. Evolution ablation shows a modest 5% decline (Cliff's δ=0.32), consistent with optimization rather than short-term survival necessity.

Quantitative coupling evidence. Time-lagged cross-correlation of per-step population means under normal conditions confirms the coupling pathways in Table 2. Energy and boundary integrity show strong anti-correlation ($r = -0.85$, $p < 0.001$, lag 0): repair continuously converts energy into boundary maintenance ($\Delta b_{\text{repair}} \propto e$), so higher boundary integrity corresponds to depleted energy reserves. Energy and internal state s_0 show strong positive correlation ($r = 0.81$, $p < 0.001$, lag 3 steps), confirming that metabolic state drives homeostatic regulation with a short delay. Boundary integrity and s_0 show moderate correlation ($r = -0.55$, $p < 0.001$, lag 3), consistent with the homeostasis→boundary pathway operating through repair efficacy.

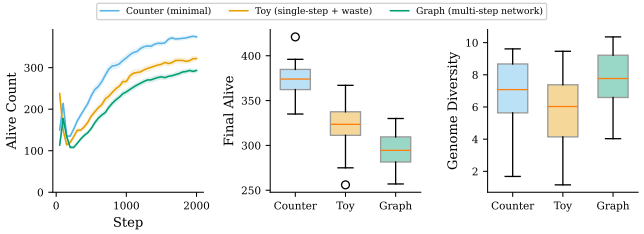

Figure 4: Proxy control comparison. Three metabolism implementations of increasing complexity on the same seeds (n=30). Graph metabolism sustains fewer organisms but higher genome diversity and waste dynamics, demonstrating that metabolic complexity produces qualitatively distinct ecological dynamics rather than simply increasing population counts.

Proxy Control Comparison

To test whether criterion ablation merely reflects tautological definitions, we compare three metabolism implementations on the same seeds (n=30): Counter (minimal single-step conversion, no waste), Toy (single-step with waste dynamics), and Graph (full multi-step network with catalytic nodes). All three satisfy "dynamic resource consumption," yet produce qualitatively different dynamics (Figure 4). Graph metabolism supports the highest genome diversity (7.58 vs. 5.69 for Toy) despite sustaining fewer organisms (293 vs. 322 for Toy, 374 for Counter), indicating that metabolic complexity imposes greater selective pressure. This confirms that the specific implementation—not merely the presence—of a criterion shapes system behavior, ruling out tautological definitions.

Pairwise Ablations and Interdependence

To test for interaction effects beyond individual necessity, we disable pairs of criteria and compute synergy: $\text{synergy}_{A,B} = \Delta_{A \cup B} - (\Delta_A + \Delta_B)$. Table 4 reports

Table 4: Pairwise ablation synergy scores (n=30 per condition, Graph metabolism). Negative synergy indicates sub-additive interaction (shared failure pathways). Baseline $\bar{x}$=293.1, consistent with Table 3.

Pair	Δ_{AB}	Exp.	Syn.	Ratio
(Metab, Homeo)	249.9	472.0	−222.0	0.53
(Metab, Resp.)	247.7	506.1	−258.4	0.49
(Reprod, Growth)	261.9	369.4	−107.5	0.71
(Bdry, Homeo)	181.9	396.2	−214.3	0.46
(Resp., Homeo)	256.4	483.9	−227.5	0.53
(Reprod, Evol)	261.9	276.7	−14.9	0.95

Exp. = Δ_A+Δ_B; Ratio = Δ_{AB}/Exp.

scores for six pairs. All show sub-additive synergy (negative), indicating shared failure pathways: individual ablations already collapse populations to near their floor (∼30–50 organisms), leaving no room for additive effects. This ceiling effect reveals that criteria damage overlapping subsystems. The (metabolism, homeostasis) pair exemplifies the shared pathway: disabling metabolism eliminates energy production, starving boundary repair ($\Delta b_{\text{repair}} \propto e$); disabling homeostasis degrades adaptive behavior, accelerating waste accumulation, which amplifies boundary decay via the waste-pressure term ($s_w \cdot w$ in Δb_{decay}). Both routes converge on boundary failure, explaining why Δ_{AB} = 249.9 falls far below the additive expectation of 472.0.

Growth–reproduction confound. The (reproduction, growth) pair confirms: $\Delta_{AB} \approx \Delta_{\text{reproduction}}$ = 261.9, so growth's effect is fully mediated through reproduction gating. This clarifies growth's role as an upstream prerequisite for reproductive competence rather than an independent viability mechanism.

Evolution Strengthening

The modest single-ablation effect of evolution (d=0.57, Cliff's δ=0.32) reflects the 2000-step simulation horizon. To demonstrate evolution's contribution at longer timescales, we run two additional experiments:

Long run. Extending simulations to 10,000 steps (n=30) yields d=1.43, Cliff's δ=0.72 ($p < 0.001$), a large effect compared to the modest 2000-step result. Normal populations reach $\bar{x}$=358.1 organisms versus 327.1 for no-evolution (Δ=−8.7%), confirming that evolutionary adaptation accumulates across generations.

Environmental shift. At step 2,500 of a 5,000-step simulation, resource regeneration rate is halved (from 0.01 to 0.005 per cell per step). Evolved populations recover more effectively ($\bar{x}$=384.6 vs. 361.4, d=1.01,

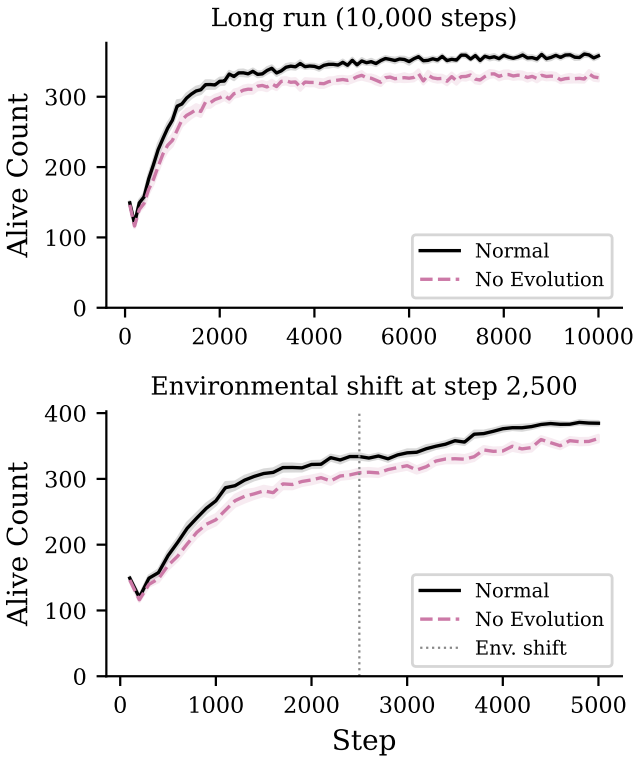

Figure 5: Evolution strengthening. Top: 10,000-step long run shows increasing divergence between normal and no-evolution conditions. Bottom: environmental shift at step 2,500 (dashed line) demonstrates evolved populations' superior recovery. Lines show mean across 30 seeds; shaded bands ±1 SEM.

Cliff's δ=0.57, $p < 0.001$), demonstrating that evolution enables adaptive response to environmental perturbation.

Homeostatic Regulation

Figure 6 shows population-mean internal state trajectories for Normal versus No Homeostasis conditions. Under normal operation, the neural-network controller actively regulates internal state variable s_0, maintaining it near 0.99 throughout the simulation (Panel A, solid). When homeostasis is disabled, s_0 decays monotonically due to the passive decay term (h_{decay} = 0.01 per step), and the population exhibits high variance as organisms lack the ability to counteract perturbations (Panel A, dashed; variance shown in Panel B). This divergence confirms that the NN-driven homeostatic mechanism constitutes an active regulatory process—not a static parameter—that satisfies the functional-analogy requirement of sustained resource consumption with measurable degradation upon removal.

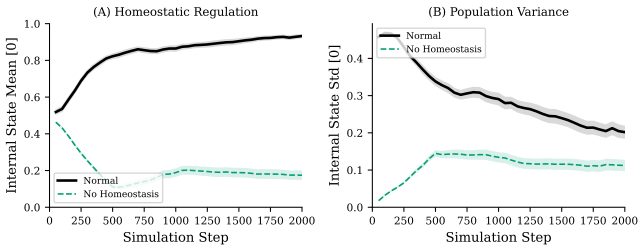

Figure 6: Homeostatic regulation trajectories (n=30). (A) Mean internal state variable s_0 over time: Normal condition (solid) maintains regulation near 0.99, while No Homeostasis (dashed) shows passive decay. (B) Population-level standard deviation of s_0: disabled homeostasis produces higher inter-organism variance. Shaded bands show ±1 SEM.

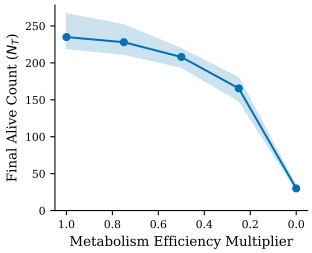

Figure 7: Graded metabolic ablation dose-response. Median final alive count (line) with IQR (shaded) across 30 seeds per level. Monotonic decline confirms continuous functional dependency ($p < 0.001$, Jonckheere-Terpstra).

Graded Metabolic Ablation

To test whether criterion ablation effects reflect a continuous functional relationship rather than a binary on/off artifact, we sweep the metabolism efficiency multiplier over $\{1.0, 0.75, 0.5, 0.25, 0.0\}$ (n=30 per level, 1,000 steps, graph metabolism). Figure 7 shows a monotonic dose-response: population viability decreases proportionally with metabolic efficiency (Jonckheere-Terpstra trend test, $p < 0.001$). This graded response demonstrates that metabolic contribution is quantitatively proportional, not merely a binary switch—partial impairment produces proportional degradation, consistent with genuine functional analogy.

Cyclic Environment

To assess whether evolved populations exhibit adaptive resilience beyond static conditions, we subject organisms to periodic resource modulation (period = 2,000 steps; high phase: 0.01, low phase: 0.005 resource per cell per step) over 10,000 steps (n=30). Figure 8 compares evolution-on versus evolution-off populations

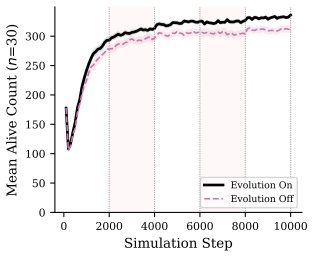

Figure 8: Cyclic environment test. Population dynamics under periodic resource modulation (period = 2,000 steps). Lightly shaded bands mark low-resource phases. Evolution-on populations recover faster after each stress phase. Lines: mean across 30 seeds; bands: ±1 SEM.

across five complete resource cycles. Evolved populations ($\bar{x}$=336.0) significantly outperform non-evolving populations ($\bar{x}$=312.6) across all cycles (d=1.10, Cliff's δ=0.58, $p < 0.001$), showing faster recovery after each low-resource phase. This demonstrates that evolutionary adaptation provides measurable resilience to recurring environmental stress, not just one-time perturbation.

Sham ablation control. To confirm that observed ablation effects are functional rather than computational artifacts, we implement a sham process that performs distance calculations matching the cost of a real criterion update but discards results. Comparing sham-on versus sham-off (n=30, 1,000 steps) yields no significant difference (Mann-Whitney U, $p > 0.05$), validating that criterion ablation effects reflect genuine functional dependencies.

Phenotype Clustering

Clustering analysis of per-seed organism traits (energy, waste, boundary integrity, genome diversity, generation count) reveals emergent phenotypic differentiation among evolved populations (Figure 9). This suggests that the evolutionary dynamics of our system produce behaviorally distinct organism strategies—an emergent property not explicitly engineered into the criteria implementation.

Discussion

Criterion interdependence. Single ablations reveal a hierarchy: reproduction, response, and metabolism form an essential triad (>84% decline), while homeostasis and boundary occupy a middle tier (∼58–77%). Pairwise ablations show uniformly sub-additive interactions (Table 4), consistent with shared failure pathways rather than independent modules—criteria converge on overlapping viability subsystems. The proxy control

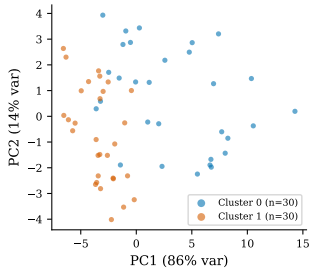

Figure 9: Phenotype clustering via PCA projection of organism trait vectors. Clusters identified by k-means (optimal k selected by silhouette score) suggest emergent behavioral strategies among evolved populations.

comparison further demonstrates that the specific implementation of a criterion shapes ecological dynamics (graph metabolism produces higher diversity but lower populations than simpler alternatives), ruling out tautological definitions.

Evolution at longer timescales. The modest 2000-step evolution effect (d=0.57, δ=0.32) grows to d=1.43 (δ=0.72) at 10,000 steps and d=1.01 (δ=0.57) under environmental perturbation, confirming that evolutionary adaptation accumulates across generations. The cyclic environment test (Figure 8) further demonstrates that evolved populations recover more rapidly from recurring resource stress, indicating adaptive resilience beyond one-time environmental shifts.

Are criteria merely engineered? One might argue that criterion ablation merely reflects system design—disabling any engineered subsystem would degrade performance. Four lines of evidence argue against this interpretation. First, the proxy control comparison shows that alternative metabolism implementations satisfying the same functional-analogy definition produce qualitatively distinct ecological dynamics (Figure 4), ruling out tautological definitions. Second, pairwise ablations reveal sub-additive interactions (Table 4), indicating shared failure pathways inconsistent with independent modules. Third, the sham ablation control (a no-op process matching real criterion computational cost) produces no significant population difference, confirming that observed effects are functional, not computational artifacts. Fourth, graded metabolic ablation produces a proportional dose-response (Figure 7), inconsistent with a binary on/off artifact.

Criterion maturity. Criteria are at varying levels of implementation maturity: five criteria (cellular organization, metabolism, homeostasis, reproduction, response) reach Level 4 (multi-process interaction), while growth and evolution are at Level 3 (dynamic single process). Evolution demonstrates heritable variation and differential survival, sufficient for functional analogy though not open-ended evolution (Level 5).

Limitations

Cellular organization is tracked via a scalar boundary-integrity variable rather than emergent spatial cohesion among swarm agents; an explicit spatial boundary model would provide a stronger functional analogy to biological membranes. Growth uses a maturation toggle that functions primarily as a reproduction gate rather than a full developmental program; a morphogenetic model would strengthen this criterion's functional-analogy claim. Evolution reaches d=1.43 at 10,000 steps but demonstrating open-ended dynamics would require 10^5+ steps with novelty metrics (Bedau et al., 2000). Scale is limited to ∼300 organisms on a single machine; larger populations might reveal emergent ecological phenomena. We adopt a weak ALife stance: this is a functional model, not a claim that digital organisms are alive.

Conclusion

We presented a testable integration of all seven textbook biological criteria as functionally interdependent processes within a single artificial life system, verified through controlled criterion-ablation, pairwise interaction, proxy control, graded ablation, and cyclic environment experiments. The functional-analogy framework—requiring dynamic operation, measurable degradation upon removal, and feedback coupling—provides a rigorous standard distinguishing genuine criteria implementations from simplified proxies.

Our results demonstrate that no criterion is decorative: removing any one causes statistically significant population decline ($p < 0.016$, Holm-Bonferroni corrected), with Cliff's δ ranging from 0.32 to 1.00. Pairwise ablations further reveal shared failure pathways—sub-additive interactions consistent with criteria converging on overlapping viability subsystems rather than operating independently.

Future work will pursue three directions: (1) a richer developmental program replacing the current growth toggle; (2) scaling to larger populations to investigate emergent ecological phenomena and open-ended evolution metrics (Bedau et al., 2000; Taylor et al., 2016); and (3) systematic environmental perturbation studies to characterize adaptive capacity across evolutionary timescales.

Code and data will be made available upon acceptance at an anonymous repository.

References

Barbieux, A. and Canaan, R. (2024). Coralai: Intrinsic evolution of embodied neural cellular automata ecosystems. In The 2024 Conference on Artificial Life, ALIFE 2024. MIT Press.

Bedau, M. A., McCaskill, J. S., Packard, N. H., Rasmussen, S., Adami, C., Green, D. G., Ikegami, T., Kaneko, K., and Ray, T. S. (2000). Open problems in artificial life. Artificial Life, 6(4):363–376.

Chan, B. W.-C. (2019). Lenia: Biology of artificial life. Complex Systems, 28(3):251–286.

Cliff, N. (1993). Dominance statistics: Ordinal analyses to answer ordinal questions. Psychological Bulletin, 114(3):494–509.

Gánti, T. (2003). The Principles of Life. Oxford University Press, Oxford.

Heinemann, C. (2008). Artificial life environment. Informatik-Spektrum, 31(1):55–61.

Holm, S. (1979). A simple sequentially rejective multiple test procedure. Scandinavian Journal of Statistics, 6(2):65–70.

Joyce, G. F. (1994). Foreword. In Deamer, D. W. and Fleischaker, G. R., editors, Origins of Life: The Central Concepts, pages xi–xii. Jones and Bartlett, Boston.

Mann, H. B. and Whitney, D. R. (1947). On a test of whether one of two random variables is stochastically larger than the other. The Annals of Mathematical Statistics, 18(1):50–60.

Maturana, H. R. and Varela, F. J. (1980). Autopoiesis and Cognition: The Realization of the Living. Boston Studies in the Philosophy and History of Science. Springer Netherlands.

McMullin, B. (2004). Thirty years of computational autopoiesis: A review. Artificial Life, 10(3):277–295.

Ofria, C. and Wilke, C. O. (2004). Avida: A software platform for research in computational evolutionary biology. Artificial Life, 10(2):191–229.

Plantec, E., Hamon, G., Etcheverry, M., Oudeyer, P.-Y., Moulin-Frier, C., and Chan, B. W.-C. (2023). Flow-lenia: Towards open-ended evolution in cellular automata through mass conservation and parameter localization. In The 2023 Conference on Artificial Life, ALIFE 2023. MIT Press.

Ray, T. S. (1991). An approach to the synthesis of life. In Langton, C. G., Taylor, C., Farmer, J. D., and Rasmussen, S., editors, Artificial Life II, volume XI of Santa Fe Institute Studies in the Sciences of Complexity, pages 371–408, Redwood City, CA. Addison-Wesley.

Ruiz-Mirazo, K., Peretó, J., and Moreno, A. (2004). A universal definition of life: Autonomy and open-ended evolution. Origins of Life and Evolution of the Biosphere, 34(3):323–346.

Taylor, T., Bedau, M., Channon, A., Ackley, D., Banzhaf, W., Beslon, G., Dolson, E., Froese, T., Hickinbotham, S., Ikegami, T., McMullin, B., Packard, N., Rasmussen, S., Virgo, N., Agmon, E., Clark, E., McGregor, S., Ofria, C., Ropella, G., Spector, L., Stanley, K. O., Stanton, A., Timperley, C., Vostinar, A., and Wiser, M. (2016). Open-ended evolution: Perspectives from the OEE workshop in York. Artificial Life, 22(3):408–423.

Urry, L. A., Cain, M. L., Wasserman, S. A., Minorsky, P. V., and Reece, J. B. (2020). Campbell Biology. Pearson, New York, 12th edition.

Yaeger, L. S. (1994). Computational genetics, physiology, metabolism, neural systems, learning, vision, and behavior or PolyWorld: Life in a new context. In Langton, C. G., editor, Artificial Life III, pages 263–298, Redwood City, CA. Addison-Wesley.